ELSEVIER

Journal of Hazardous Materials B137 (2006) 1016–1024

Journal of Hazardous Materials

www.elsevier.com/locate/jhazmat

Photodegradation of orange I in the heterogeneous iron oxide–oxalate complex system under UVA irradiation

Jing Lei [a,b], Chengshuai Liu [b,c], Fangbai Li [b,*], Xiaomin Li [b,c], Shungui Zhou [b], Tongxu Liu [b,c], Minghua Gu [a], Qitang Wu [d]

[a] *The Faculty of Agriculture, Guangxi University, Nanning 630005, PR China*

[b] *Guangdong Key Laboratory of Agricultural Environment Pollution Integrated Control, Guangdong Institute of Eco-Environment and Soil Sciences, Guangzhou 510650, PR China*

[c] *Guangzhou Institute of Geochemistry, Chinese Academy of Sciences, Guangzhou 510640, PR China*

[d] *College of Natural Resources and Environment, South China Agricultural University, Guangzhou 510642, PR China*

Received 24 December 2005; received in revised form 15 March 2006; accepted 15 March 2006

Available online 22 May 2006

Abstract

To understand the photodegradation of azo dyes in natural aquatic environment, a novel photo-Fenton-like system, the heterogeneous iron oxide–oxalate complex system was set up with the existence of iron oxides and oxalate. Five iron oxides, including γ-FeOOH, IO-250, IO-320, IO-420 and IO-520, were prepared and their adsorption capacity was investigated in the dark. The results showed that the saturated adsorption amount (Γ_{max}) was ranked the order of IO-250 > IO-320 > γ-FeOOH > IO-420 > IO-520 and the adsorption equilibrium constant (K_a) followed the order of IO-250 > IO-520 > γ-FeOOH > IO-420 > IO-320. The effect of initial pH value, the initial concentrations of oxalate and orange I on the photodegradation of orange I were also investigated in different iron oxide–oxalate systems. The results showed that the photodegradation of orange I under UVA irradiation could be enhanced greatly in the presence of oxalate. And the optimal oxalate concentrations (C^0_{ox}) for γ-FeOOH, IO-250, IO-320, IO-420 and IO-520 were 1.8, 1.6, 3.5, 3.0 and 0.8 mM, respectively. The photodegradation of orange I in the presence of optimal C^0_{ox} was ranked as the order of γ-FeOOH > IO-250 > IO-320 > IO-420 > IO-520. The optimal range of initial pH was at about 3–4. The first-order kinetic constant for the degradation of orange I decreased with the increase in the initial concentration of orange I. Furthermore, the variation of pH, the concentrations of Fe^{3+} and Fe^{2+} during the photoreaction were also strongly dependent on the C^0_{ox} and iron oxides.

Keywords: Iron oxide; Oxalate; Azo dye; Photodegradation; Photo-Fenton

1. Introduction

Dye pollutants produced from the textile industries are becoming a major source of environmental contaminations [1]. Approximately 150 tonnes everyday is estimated to be released into the aquatic environment all over the world [2]. The release of those dyes in the aquatic environment is a considerable source of non-aesthetic pollution and these dyes are also resistant to aerobic degradation, and under anaerobic conditions the dyes can be transformed into carcinogenic aromatic amines [3,4].

Fenton reaction is known to be a very effective way in the removal of organic pollutants for wastewater treatment [5–7]. Hydroxyl radicals (•OH) with high reactivity can form during Fenton reaction and degrade most of organic compounds with second-order rate constants of 10^8–10^{10} M^{-1} s^{-1} [8–10]. When light was introduced into Fenton or Fenton-like system, as called photo-Fenton and photo-Fenton-like reactions, more •OH could be generated [11]. In the last decade, photo-Fenton and photo-Fenton-like reactions have been extensively utilized to degrade azo dyes [12–15]. However, sufficient H_2O_2 have to be added to make the system efficient because H_2O_2 is the direct source of •OH in traditional Fenton system [16,17]. But H_2O_2 is an acute reactive reagent and cannot stand in nature for a long time. The application of Fenton and Fenton-like system for the degradation of azo dyes in natural aquatic environment was limited.

It is noticeable that heterogeneous catalytic process at mineral surfaces should be vital for organic pollutants degradation in surface soil and surface water [18–20]. Iron oxides (including oxy-

* Corresponding author. Tel.: +86 20 87024721; fax: +86 20 87024123.
E-mail address: cefbli@soil.gd.cn (F. Li).

0304-3894/$ – see front matter © 2006 Elsevier B.V. All rights reserved.
doi:10.1016/j.jhazmat.2006.03.028

hydroxides) should be a kind of natural minerals and exist in the earth's crust with great content (5.1 mass%) [21]. Most of iron oxides show semiconductor properties with narrow band gap (2.0–2.3 eV) and should be photoactive under solar irradiation as photocatalysts [22]. To be more important, iron oxide coexist with oxalate can set up a photo-Fenton-like system and $^{\bullet}OH$ can be produced without external H_2O_2 [23,24]. Oxalic acid comes from the secretion of plants in natural environment [25] and also forms as an intermediate in the catalytic oxidation of phenol [26]. In a word, this Fenton-like process can utilize natural materials (iron oxides and oxalic acid) without additional H_2O_2 and artificial injection of iron. It is meaningful to investigate the photochemical reaction in the iron oxide–oxalate complex system for understanding the degradation of azo dyes in natural surface water. In fact, the photochemistry of Fe(III)–oxalate complexes in natural aquatic environment, fog, precipitation, tropospheric aerosols and soil solution has received considerable attention over the past 3 decades [27–30] because iron oxide–oxalate exhibit a strong ligand-to-metal charge transformation ability. But, to our best knowledge, there is little report on the photodegradation of azo dyes in the system consisting of iron oxide minerals and oxalic acid.

The objectives of this study were to investigate the effect of iron oxides, pH value, the initial concentration of oxalic acid and the initial concentration of orange I on the photodegradation of orange I, and also to study the effects of iron oxides and initial concentration of oxalic acid on the variation of the pH value and the formation of Fe^{2+} and Fe^{3+} during the photochemical process.

2. Experimental

2.1. Preparation and characterization of iron oxides

γ-FeOOH was prepared by hydrothermal method and IO-250, IO-320, IO-420 and IO-520 were obtained by sintering the prepared γ-FeOOH at 250, 320, 420 and 520 °C, respectively for 2 h, which was reported in our previous study [31]. To determine the crystal phase composition of the iron oxides, X-ray diffraction (XRD) measurement was carried out at room temperature using a Rigaku D/MAX-IIIA diffractometer with Cu Kα radiation. The accelerating voltage of 35 kV and emission current of 30 mA were used. The total surface area and total pore volume were measured by the Brunauer–Emmett–Teller (BET) method using a Coulter SA-3100, in which the N_2 adsorption at 77 K was applied and a Carlo Erba sorptometer was used.

2.2. Adsorption isotherm experiment

Adsorption of orange I on the iron oxides was determined by using the batch experiment in the dark. A fixed amount of the iron oxides (0.1 g) was added to 10 mL of orange I solution with varying concentrations in glass tubes, which were agitated for 24 h at 130 rpm in a thermostatic shaker bath and maintained at a temperature of 25 ± 1 °C. The concentrations of orange I were measured by UV–vis spectrometer and the adsorbed amount of orange I on the iron oxide was calculated based on a mass balance.

2.3. Set up of photochemical reactor

All photoreaction experiments were carried out in a photochemical reactor system, which consist of a Pyrex cylindrical reactor vessel with an effective volume of 250 mL, a cooling water jacket, two aeration inlet and an 8-W black light lamp (Luzchem Research Inc.) positioned axially at the center as a UVA light source with a main emission at 365 nm. The reaction temperature was kept at 25 ± 1 °C by cycling water and the reaction suspension was constantly stirred by placing the reactor on a magnetic stirrer during the reaction process.

2.4. Photochemical experimental procedure

The reaction suspension was prepared by adding given dosage of iron oxide powder into 250 mL of orange I solution or mixed solution of orange I and oxalic acid. Prior to photoreaction, the suspension was magnetically stirred in a dark condition for 30 min to establish an adsorption/desorption equilibrium status. The suspension was then irradiated by UVA light with the intensity of 600 mW/cm^2, which was measured by a UVA radiation meter (Photoelectric Instrument Factory of Beijing Normal University) with a sensor of 365 nm, and continuously aerated with the dissolved oxygen (DO) concentration of about 11.8 mg/L, which was measured by a dissolved oxygen meter, Model 9173R made in China. At given time intervals, the analytical samples were taken from the suspension and immediately centrifuged at 4500 rpm for 20 min. The supernatant was transferred and stored in the dark for analysis.

2.5. Analytical methods

To measure orange I concentration, a UV–vis spectrophotometer (UV–vis TU-1800, Purkinje General, Beijing) was used to determine the absorbance of orange I at a wavelength of 497 nm. Prior to the measurement, a calibration curve was obtained using standard orange I solution (from 0 to 20 mg/L) and a good linear relationship was shown between absorbance and orange I concentration. The concentration of Fe^{3+} and Fe^{2+} were determined by the 1,10-phenanthroline method [32]. Total organic carbon (TOC) analysis was carried out by means of a Shimadzu TOC-V CPH total organic carbon analyser.

3. Results and discussions

3.1. Characteristics of iron oxides

The results of detailed analysis of XRD and BET were shown in our previous study [31] and they are listed in Table 1. IO-250 and IO-320 had the mixed crystal structure of γ-Fe_2O_3 and α-Fe_2O_3 and the content of α-Fe_2O_3 in IO-320 was higher than in IO-250. IO-420 and IO-520 had a pure α-Fe_2O_3 crystal structure. The BET results showed that the total surface area decreased with increase in sintering temperature. IO-320 had

Table 1
The crystal structure, total surface area, micropore surface area and total pore volume of iron oxides

Iron oxides	γ-FeOOH	IO-250	IO-320	IO-420	IO-520
Crystal structure	γ-FeOOH	γ-Fe_2O_3/α-Fe_2O_3	γ-Fe_2O_3/α-Fe_2O_3	α-Fe_2O_3	α-Fe_2O_3
Total surface area (m^2/g)	130.53	85.34	69.66	32.33	22.11
Total pore volume (m^3/g)	0.2977	0.3485	0.3762	0.2747	0.1650

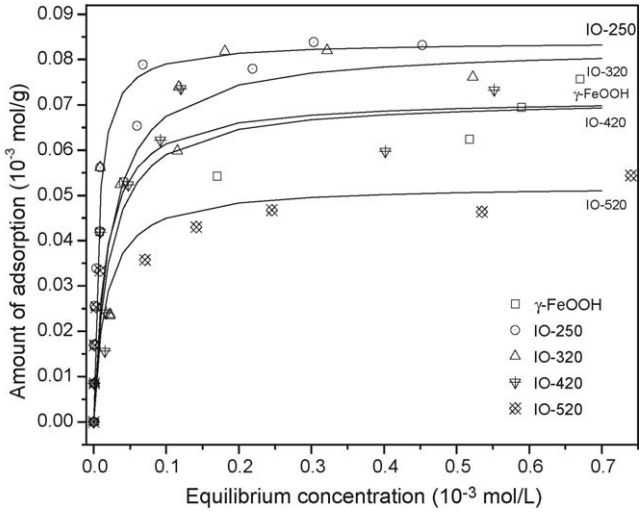

Fig. 1. The adsorption isotherms of orange I on the surface of different iron oxides obtained by plotting the equilibrium concentration (C_e) vs. the adsorbed amounts of orange I (Γ).

the highest total pore volume of 0.3762 m^3/g and the total pore volumes of γ-FeOOH, IO-250, IO-420 and IO-520 were 0.2977, 0.3485, 0.2747 and 0.1650 m^3/g, respectively.

3.2. The adsorption behavior of iron oxides

The adsorption isotherms of orange I on the different iron oxides by plotting C_e/Γ versus C are shown in Fig. 1, which are well fitted by the Langmuir adsorption model as Eq. (1).

$$\frac{C_e}{\Gamma} = \frac{1}{\Gamma_{max}} \cdot C_e + \frac{1}{K_a \cdot \Gamma_{max}} \quad (1)$$

where C_e is the equilibrium concentration in the solution in M, K_a the adsorption equilibrium constant in L/mol and Γ_{max} is the saturated adsorption capacity in mol/g. The saturated adsorption amount (Γ_{max}) and the adsorption equilibrium constant (K_a) of orange I onto different iron oxides are listed in Table 2. The saturated adsorption amount (Γ_{max}) of iron oxides was ranked as the order of IO-250 > IO-320 > γ-FeOOH > IO-420 > IO-520 while the adsorption equilibrium constant (K_a) was ranked as the order of IO-250 > IO-520 > γ-FeOOH > IO-420 > IO-320. The adsorption ability should be influenced by the physical and chemical properties of the iron oxides. The large amount of the specific surface area and total pore volume would be beneficial to achieve better physical adsorption [33]. But the BET results showed that the specific surface area should follow the order of γ-FeOOH > IO-250 > IO-320 > IO-420 > IO-520 while IO-320 and IO-250 had the higher total pore volume. This implies that the chemical adsorption should exist between orange I and iron oxides. Nadtochenko and Kiwi [34] reported the complex ($Fe^{3+}\cdots$orange II) could form between Fe^{3+} and orange II. It was believed that the complex ($Fe^{3+}\cdots$orange I) could form between Fe^{3+} and orange I by chemical adsorption owing to their similar chemical structure. A larger K_a value should be attributed to the stronger chemical adsorption.

Table 2
The saturated adsorption amount (Γ_{max}) and adsorption equilibrium constant (K_a) of orange I by using different iron oxides

Iron oxide	$\Gamma_{max} \times 10^{-5}$ (mol/g)	$K_a \times 10^5$ (L/mol)	R
γ-FeOOH	7.14	0.61	0.993
IO-250	8.39	1.61	0.999
IO-320	8.28	0.44	0.994
IO-420	7.13	0.48	0.989
IO-520	5.22	0.62	0.995

3.3. The dependence of the photodegradation of orange I on the initial concentration of oxalate

The initial concentration of oxalate (C^0_{ox}) should be a key factor to affect the photodegradation of orange I in iron oxide–oxalate system. To study the effect of the C^0_{ox} on the photodegradation of orange I, a set of experiments with initial orange I concentration of 20 mg/L and iron oxides dosage of 0.5 g/L were carried out under UVA irradiation, followed by the experiments on different C^0_{ox} in the range of 0–5.0 mM without pH control. Fig. 2 shows the dependence of orange I photodegradation on the C^0_{ox} under UVA light irradiation. Obviously, when there was no oxalic acid in the suspension, orange I was only degraded slightly. In the absence of oxalate, iron oxides acted as a photocatalyst and could be excited to generate electron–hole pairs [35], although orange I was degraded at a low k value. In the presence of oxalate, iron oxide–oxalate complex formed and a photo-Fenton-like system was set up. It was confirmed that the presence of iron oxide and oxalate in cooperation can greatly accelerate the degradation of orange I. The experimental data were well fitted by the first-order kinetic model and the first-order kinetic constant (k) for the photodegradation of orange I are listed in Table 3. The results in Fig. 2 and Table 3 show that the orange I degradation depended strongly on the C^0_{ox}. In the low range, the orange I degradation was increased significantly with the increase of C^0_{ox}, but was inhibited greatly with an excessive amount of oxalate. Obviously, there should be an optimal amount of oxalate to achieve the best performance of the photodegradation of orange I. The optimal C^0_{ox} was at 1.8, 1.6, 3.5, 3.0 and 0.8 mM level and the corresponding k values were 1.72×10^{-2}, 1.66×10^{-2}, 1.62×10^{-2}, 1.36×10^{-2} and 0.92×10^{-2} min^{-1} by using γ-FeOOH, IO-250, IO-320, IO-420

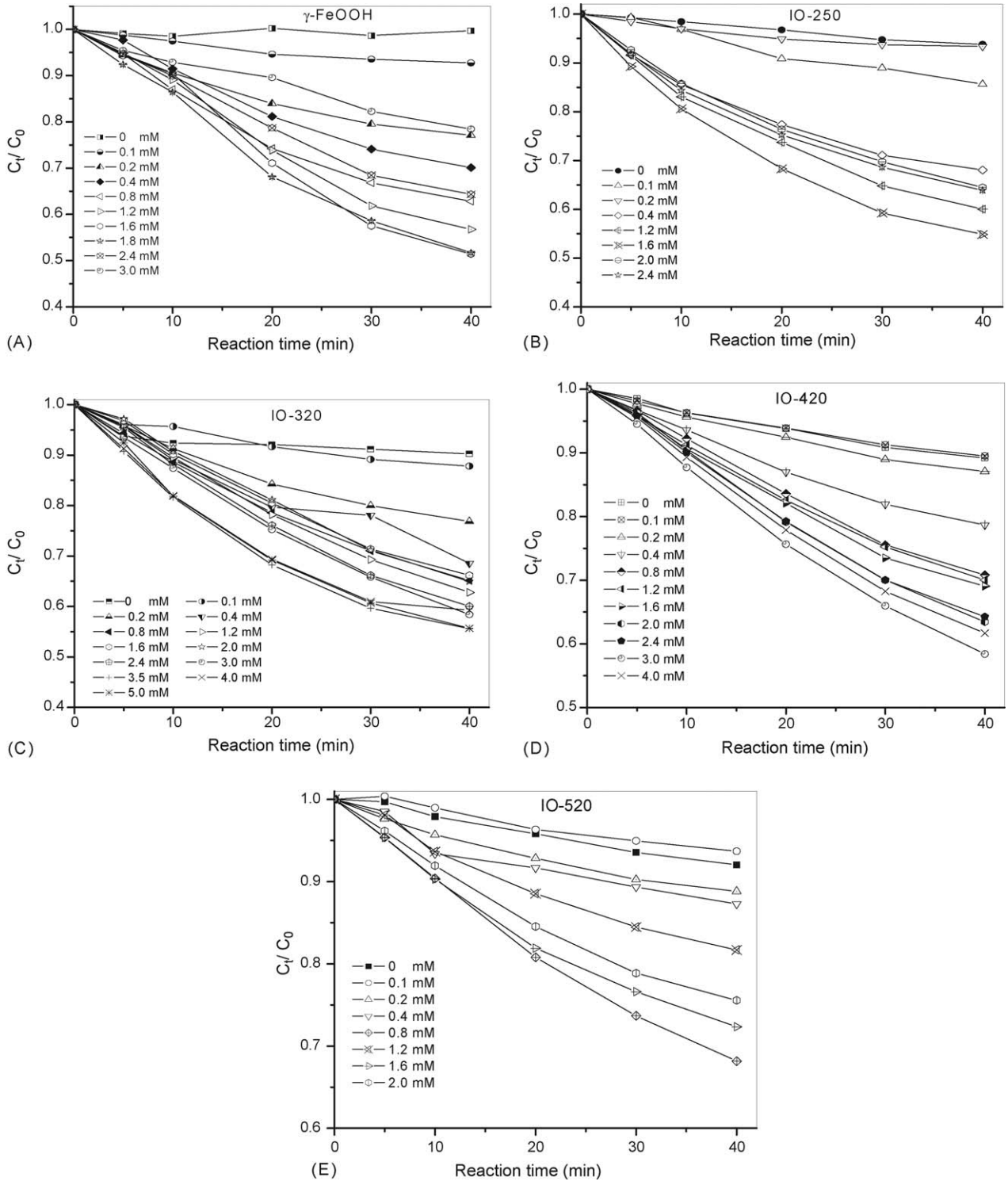

Fig. 2. The effect of the C_{ox}^{0} on the photodegradation of orange I, with the initial concentration of 20 mg/L under UVA light irradiation by using 0.5 g/L γ-FeOOH (A), IO-250 (B), IO-320 (C), IO-420 (D), and IO-520 (E).

and IO-520, respectively.

In order to understand the photoreaction process of orange I degradation in iron oxide–oxalate system, the interaction of iron oxide and oxalate under UVA light irradiation was discussed. On the surface of iron oxides, oxalic acid is first adsorbed by iron oxide particles to form iron oxide–oxalate complexes of $[\equiv Fe^{III}(C_2O_4)_n]^{3-2n}$ as described by Eq. (2). $[\equiv Fe^{III}(C_2O_4)_n]^{3-2n}$ can be excited to form $[\equiv Fe^{II}(C_2O_4)_{(n-1)}]^{4-2n}$ and oxalate radical $(C_2O_4)^{\bullet -}$ as indicated by Eq. (3). In the solution, $[Fe^{III}(C_2O_4)_n]^{3-2n}$ could be also excited to form $[Fe^{II}(C_2O_4)_{(n-1)}]^{4-2n}$ and oxalate radical $(C_2O_4)^{\bullet -}$ as described by Eq. (4). The oxalate radical

Table 3
The apparent first-order kinetic constant ($k \times 10^{-2}$ min^{-1}) and relation coefficient (R) for degradation of orange I with different initial concentration of oxalic acid ($n = 6$, Significance > 0.99 if $R > 0.874$)

C_{ox} (mM)	γ-FeOOH		IO-250		IO-320		IO-420		IO-520	
	k	R	k	R	k	R	k	R	k	R
0.0	0.003	0.6700	0.16	0.9960	0.18	0.7949	0.27	0.9929	0.21	0.9944
0.1	0.24	0.9880	–	–	0.37	0.9776	0.29	0.9950	0.17	0.9901
0.2	0.73	0.9829	0.24	0.9848	0.72	0.9880	0.37	0.9950	0.33	0.9884
0.4	0.94	0.9922	1.08	0.9809	0.94	0.9852	0.55	0.9958	0.36	0.9896
0.8	1.27	0.9885	–	–	1.12	0.9978	0.89	0.9977	0.92	0.9981*
1.2	1.47	0.9942	1.39	0.9912	1.19	0.9984	0.92	0.9987	–	–
1.6	1.70	0.9923	1.66	0.9882**	1.06	0.9968	0.97	0.9940	0.87	0.9931
1.8	1.72	0.9951*	–	–	–	–	–	–	–	–
2.0	–	–	1.18	0.9921	1.08	0.9978	1.12	0.9948	0.75	0.9937
2.4	1.12	0.9948	1.23	0.9880	1.31	0.9976	1.13	0.9980	–	–
3.0	0.62	0.9934	–	–	1.37	0.9994	1.36	0.9994*	–	–
3.5	–	–	–	–	1.62	0.9867**	–	–	–	–
4.0	–	–	–	–	1.51	0.9760	0.64	0.9986	–	–

* $P < 0.01$.
** $P \leq 0.01$.

can be transferred into carbon-centered radical $(CO_2)^{\bullet -}$ as described by Eq. (5); and the excited electron is transferred from carbon-centered radical into adsorbed oxygen and superoxide ion ($O_2^{\bullet -}$), as described by Eq. (6). Fe^{3+} reacts with $O_2^{\bullet -}$ to form O_2 and Fe^{2+} as described by Eq. (7) and Fe^{2+} reacts with $O_2^{\bullet -}$ to form H_2O_2 in acidic solution and Fe^{3+} as described by Eq. (8). To be important, Fe^{2+} is re-oxidized to Fe^{3+} in the presence of O_2. Fe^{2+} reacts with H_2O_2 to form hydroxyl radical ($^{\bullet}OH$) and Fe^{3+} as described by Eq. (9). The iron oxide–oxalate complex includes $[\equiv Fe^{III}(C_2O_4)_n]^{3-2n}$ or $[\equiv Fe^{II}(C_2O_4)_{(n-1)}]^{4-2n}$ on the surface and $Fe^{III}(C_2O_4)_n{}^{3-2n}$ or $[Fe^{II}(C_2O_4)_{(n-1)}]^{4-2n}$ in solution, which are much more photoactive than the other Fe^{3+} species. Therefore, the degradation of orange I could be efficiently enhanced with certain amounts of oxalate and be promoted greatly with the increase of oxalate concentration. This was the reason why the photodegradation of orange I was enhanced greatly in the presence of oxalate. However, excessive oxalate would occupy the adsorbed sites on the surface of iron oxide and react competitively for hydroxyl radical ($^{\bullet}OH$). The adsorption of orange I on the surface was also hindered and only a part of hydroxyl radical would be utilized by orange I.

$$\text{Iron oxide} + nH_2C_2O_4 \leftrightarrow [\equiv Fe(C_2O_4)_n]^{(2n-3)-} \quad (2)$$

$$[\equiv Fe(C_2O_4)_n]^{(2n-3)-} + h\nu \rightarrow Fe(C_2O_4)_2{}^{2-}(\text{or} \equiv Fe(C_2O_4)_2{}^{2-}) + CO_2{}^{\bullet -} \quad (3)$$

$$Fe^{III}(C_2O_4)_n{}^{3-2n} + h\nu \rightarrow [Fe^{II}(C_2O_4)_{(n-1)}]^{4-2n} + C_2O_4{}^{\bullet -} \quad (4)$$

$$C_2O_4{}^{\bullet -} \rightarrow CO_2 + CO_2{}^{\bullet -} \quad (5)$$

$$CO_2{}^{\bullet -} + O_2 \rightarrow CO_2 + O_2{}^{\bullet -} \quad (6)$$

$$O_2{}^{\bullet -} + Fe^{3+} \rightarrow Fe^{2+} + O_2 \quad (7)$$

$$O_2{}^{\bullet -} + nH^+ + Fe^{2+} \rightarrow Fe^{3+} + H_2O_2 \quad (8)$$

$$Fe^{2+} + H_2O_2 \rightarrow Fe^{3+} + OH^- + {}^{\bullet}OH \quad (9)$$

3.4. The effect of initial pH value

To investigate the effect of initial pH value on the photodegradation of orange I, a set of experiments were carried out under different initial pH, which was adjusted by titrating NaOH or $HClO_4$ before reaction, with initial concentration of orange I of 20 mg/L and iron oxides dosage of 0.5 g/L. And the initial concentration of oxalic acid was the optimal C_{ox}^0 of 1.8 mM for γ-FeOOH and the optimal C_{ox}^0 of 3.5 mM for IO-320. The dependence of the first-order kinetic constant k values on initial pH value is shown in Fig. 3. The results showed that the

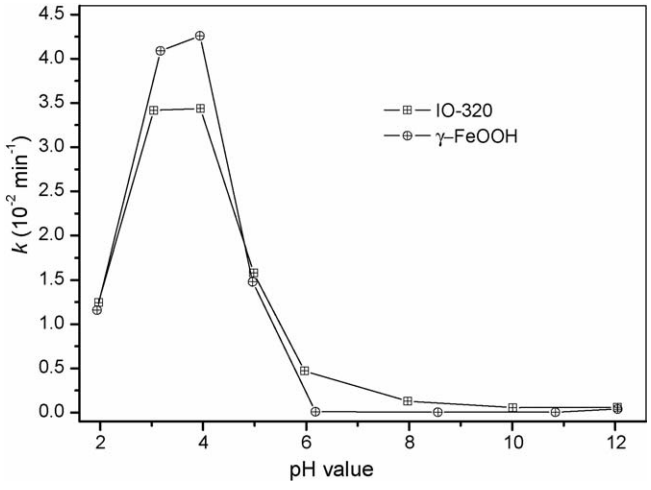

Fig. 3. The dependence of the first-order kinetic constant k value for the degradation of orange I on the initial pH value by using 0.5 g/L γ-FeOOH and IO-320 with the corresponding optimal C_{ox}^0 in the presence of 20 mg/L orange I under UVA light irradiation.

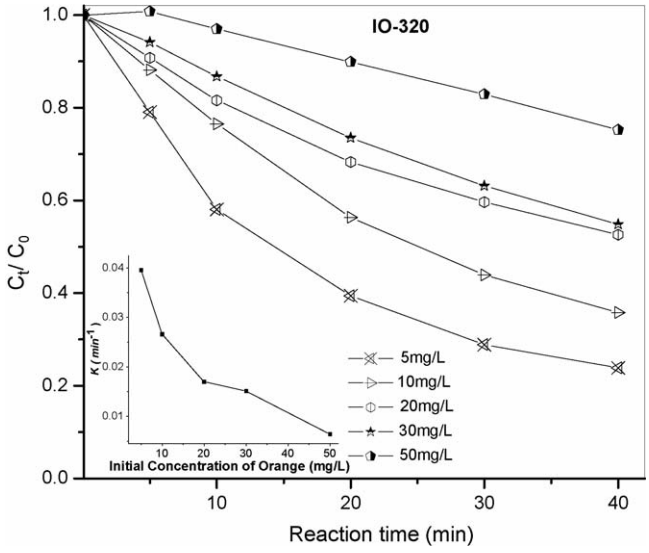

Fig. 4. The effect of the initial concentration of orange I on its degradation under UVA light irradiation by using 0.5 g/L IO-320 and 3.5 mM C_{ox}^0.

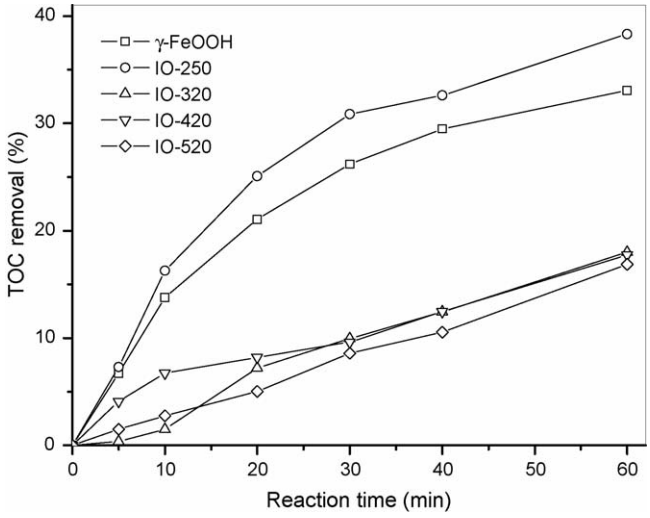

Fig. 5. The TOC removal during the photoreaction in the presence of 20 mg/L orange I by using 0.5 g/L iron oxides and 1.6 mM C_{ox}^0 under UVA light irradiation.

photodegradation of orange I should depend strongly on pH value. Obviously, there was an optimal range of initial pH value for the photodegradation of orange I. For IO-320, the k values were 3.42×10^{-2} and 3.44×10^{-2} min^{-1} at pH value of 3.04 and 3.95, respectively, while those were 4.09×10^{-2} and 4.26×10^{-2} min^{-1} at pH value of 3.17 and 3.94, respectively for γ-FeOOH. The degradation of orange I would be inhibited significantly when the initial pH values were beyond the range of about 3–4, and especially, orange I was almost not degraded when the initial pH value was above 6. Obviously, the initial pH value should be a very important factor affecting this photo-Fenton-like reaction and the optimal initial pH value for the photodegradation of orange I was at 3–4.

Balmer and Sulzberger [28] had reported that when the pH was at around 4, the main Fe(III)–oxalate species were $Fe^{III}(C_2O_4)_2^-$ and $Fe^{III}(C_2O_4)_3^{3-}$, which are highly photoactive. And in our experiment, the iron oxide–oxalate complex system at pH value of about 3–4 might have a higher concentration of $Fe^{III}(C_2O_4)_2^-$ and $Fe^{III}(C_2O_4)_3^{3-}$ and then more $^{\bullet}OH$ would be generated. When the pH value increased to about 4–5, Fe(III)–oxalate species were mainly $Fe^{III}(C_2O_4)^+$, which was low photoactive. And when the pH value was up to 6, the Fe^{3+} and Fe^{2+} almost cannot exist in the solution and the predominant Fe(III) and Fe(II) species were Fe(II)–OH and Fe(III)–OH as the precipitate, which might hardly be photoactive. So the orange I almost could not be degraded when the pH value was above 6.

3.5. The effect of initial concentration of orange I

To investigate the effect of initial concentration of orange I on its degradation, a set of experiments were carried out with initial concentration of orange I varying from 5 to 50 mg/L in the presence of 3.5 mM C_{ox}^0 by using IO-320 with the dosage of 0.5 g/L under UVA irradiation. The results are shown in Fig. 4. And the inserted figure therein shows the dependence of the first-order kinetics constants (k) on the initial concentration of orange I. The results showed that the k values should decrease significantly with the increase in the initial concentration of orange I. The k values were 3.96×10^{-2}, 2.67×10^{-2}, 1.70×10^{-2}, 1.51×10^{-2} and 0.64×10^{-2} min^{-1} when the initial concentration of orange I were 5, 10, 20, 30 and 50 mg/L, respectively.

3.6. Mineralization of orange I

The mineralization of orange I denoted as TOC removal is shown in Fig. 5. The experiments were conducted with 0.5 g/L iron oxides and 1.6 mM C_{ox}^0 in the presence of the initial concentration of orange I of 20 mg/L under UVA light irradiation. The removal percentage for TOC was 33.1%, 38.3%, 18.0%, 17.7% and 16.9% for γ-FeOOH, IO-250, IO-320, IO-420 and IO-520 after 60 min reaction. It should be pointed out that the initial TOC in the solution should contain orange I and oxalic acid.

3.7. The variation of pH value

In this investigation, the test of pH value during the reaction was also conducted to investigate the dependence of the change of pH value on the C_{ox}^0. The change of pH values with reaction time is plotted in Fig. 6. Fig. 6A shows the variation of pH value by using 0.5 g/L IO-320 in the presence of different C_{ox}^0. The pH value increased significantly from 3.90, 3.20, 2.97, 2.72, 2.62 and 2.40 before photoreaction to 4.47, 4.89, 5.16, 5.32, 5.38 and 5.35 after 40 min photoreaction when the C_{ox}^0 were 0.2, 0.8, 1.6, 2.4, 3.5 and 5.0 mM, respectively. The increase of pH value was mainly attributed to the dissolution of iron oxides and the formation of OH^- as described by Eq. (9). Obviously, a higher C_{ox}^0 led to a lower initial pH value. And the increased amount of pH value of the solution in the presence of a higher C_{ox}^0 was much more than in the presence of a lower C_{ox}^0. At the meantime, the variation of pH value in the presence of 1.6 mM C_{ox}^0 was also dependent on the different iron oxides,

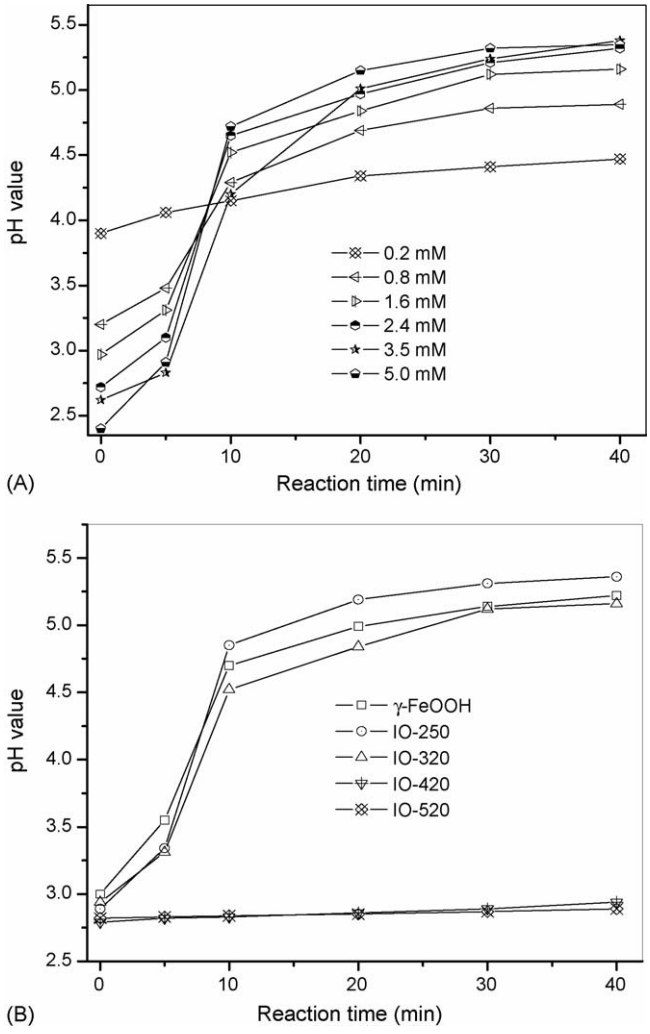

Fig. 6. The dependence of the variation of pH value on C_{ox}^{0} by using 0.5 g/L IO-320 (A) and on different iron oxides with the dosages of 0.5 g/L at the presence of 1.6 mM C_{ox}^{0} (B) under UVA light irradiation.

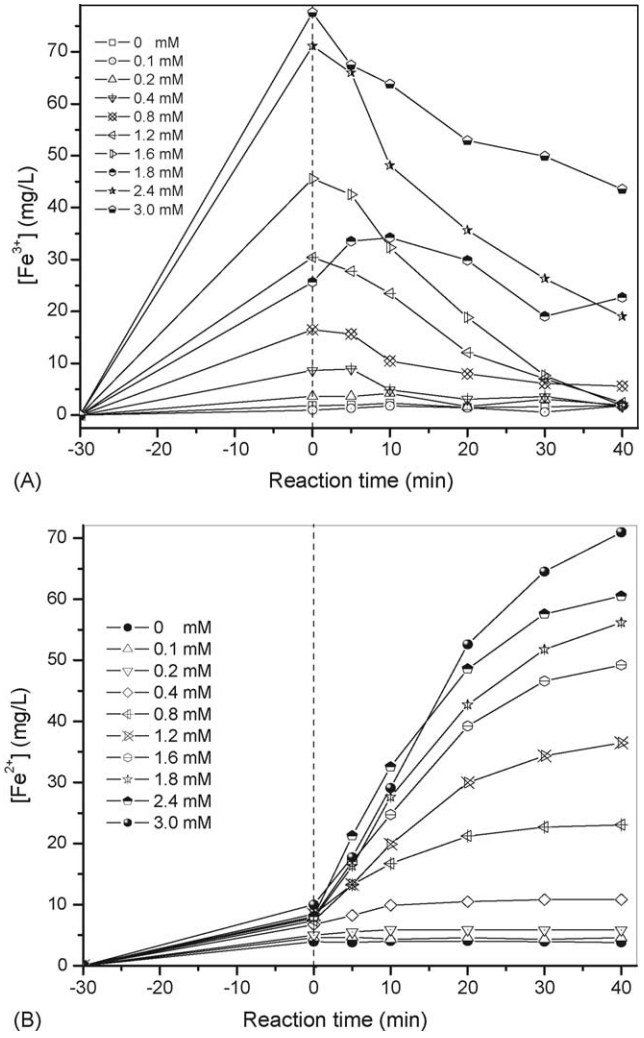

Fig. 7. The concentration of the dissolved Fe^{3+} (A) and Fe^{2+} (B) vs. reaction time with different C_{ox}^{0} by using 0.5 g/L γ-FeOOH under UVA light irradiation.

as showed in Fig. 6B. The pH value increased significantly from 3.00, 2.89 and 2.94 before photoreaction to 4.70, 4.85 and 4.52, respectively after 10 min irradiation, and then increased slowly to 5.22, 5.36 and 5.16 after 40 min during the photoreaction for γ-FeOOH, IO-250 and IO-320, respectively. However, the pH values were steady-going at about 2.8 during the photoreaction for IO-420 and IO-520 because these two iron oxides had higher thermodynamics stability and it is difficult to be dissolved by H^{+} and only a little dissolved Fe^{3+} formed. Fig. 6B shows that the initial pH value was less than 3 when C_{ox}^{0} was up to 1.6 mM. As above-mentioned, a lower pH value was not favorable to the photodegradation of orange I. Therefore, the photodegradation should be inhibited by excessive oxalate.

3.8. The formation of Fe^{2+} and Fe^{3+}

During the photoreaction, iron oxides would be photo-dissolved. And the oxalate could greatly enhance the dissolution of iron oxides under UVA light irradiation, as shown in Fig. 7, which showed the change of the concentration of Fe^{3+} (A) and Fe^{2+} (B) in the presence of different C_{ox}^{0} by using 0.5 g/L γ-FeOOH under UVA light irradiation. During the photo-dissolution of iron oxides, dissolved Fe^{3+} species could be photo-reduced to generate Fe^{2+} species. Obviously, the concentration of Fe^{2+} and Fe^{3+} in the reaction solution depended strongly on the C_{ox}^{0}. Higher C_{ox}^{0} led to higher concentration of Fe^{2+} and Fe^{3+}. Fig. 7A shows that the concentration of Fe^{3+} dramatically increased and reached the peak after 30 min dark adsorption in the solution while the concentration of Fe^{2+} were negligible at the same time as shown in Fig. 7B. The results showed that iron oxides can be quickly dissolved in oxalic acid solution and the reduction process of Fe^{3+} happened slightly in the dark. The concentration of Fe^{3+} always kept decreasing while the concentration of Fe^{2+} kept obviously increasing during the whole photoreaction. The decrease of the concentration of Fe^{3+} might be attributed to the precipitation and photo-reduction. Firstly, the pH value gradually increased due to the degradation of oxalic acid, and Fe^{3+} precipitated as $Fe(OH)_3$ with the increase of pH value. Secondly, Fe^{3+} species can be easily reduced under UVA light irradiation and Fe^{2+} could be produced during the reaction even though Fe^{2+} would be consumed and

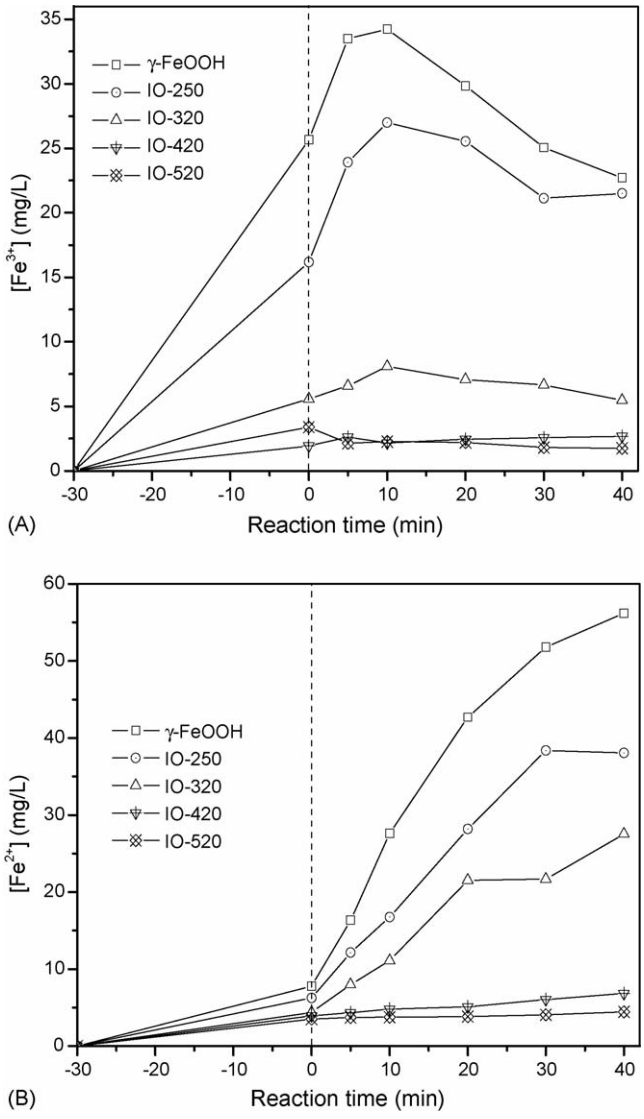

Fig. 8. The concentration of the dissolved Fe^{3+} (A) and Fe^{2+} (B) vs. reaction time by using different iron oxides with the dosages of 0.5 g/L at the presence of 1.6 mM C_{ox}^0 under UVA light irradiation.

Fe^{3+} formed in order to compensate Fe^{3+} because of the precipitation of Fe^{3+}, based on the Fenton-like reaction (Eqs. (8) and (9)). So the concentration of Fe^{2+} increased at slow rate in the later stage of the photoreaction. By the way, excessive oxalate would lead to the formation of a large amount of Fe^{3+}, which would inhibit the formation of H_2O_2, as described in Eq. (8). Therefore, the excessive concentration of Fe^{3+} was also harmful to the photodegradation of orange I. This should be another reason why excessive oxalate would lead to the inhibition of the photodegradation of orange I in the system.

Fig. 8 shows that the concentration of Fe^{2+} and Fe^{3+} in the iron oxide–oxalate system also depended on the iron oxides. The concentration of Fe^{3+} increased dramatically at the first 10 min for γ-FeOOH, IO-250 and IO-320 during the photoreaction and reached the peak value of 34.2, 27.0 and 8.08 mg/L, respectively, and then, decreased gradually with the reaction time while for IO-420 and IO-520, the concentration of Fe^{3+} remained stable after 30 min dark adsorption, as shown in Fig. 8A. And the concentration of Fe^{2+} increased gradually for γ-FeOOH, IO-250 and IO-320 during the photoreaction while kept always below 7 mg/L for IO-420 and IO-520 during the whole photoreaction, as shown in Fig. 8B. IO-420 and IO-520 with pure α-Fe_2O_3 phase had the more thermodynamics stability and lower specific surface area than IO-250 and IO-320 which had the mixed phase of γ-Fe_2O_3 and α-Fe_2O_3, and than γ-FeOOH phase [36]. It is difficult to form ≡Fe(III)–oxalate complexes on the surface of IO-420 and IO-520, and then the concentration of dissolved iron in the solution was at low level. The formation of Fe^{3+} and Fe^{2+} during the reaction had important effects on the degradation of orange I. The amount of dissolved Fe^{3+} in the suspension of γ-FeOOH, IO-250, IO-320 was much more than in the suspension of IO-420 and IO-520. More dissolved Fe^{3+} led to higher concentration of Fe(III)–oxalate complex, and then that would result in higher efficiency for the degradation of orange I. The lower concentration of ≡Fe(III)–oxalate complexes on the surface of iron oxides and Fe(III)–oxalate in the solution for IO-420 and IO-520 led to a lower photochemical activity for the degradation of orange I.

4. Conclusions

The heterogeneous iron oxide–oxalate complex system, as a photo-Fenton-like system, was set up in the presence of iron oxide and oxalate together. Orange I could be effectively degraded in the system under UVA irradiation. The photodegradation of orange I depended strongly on the types of iron oxides, the initial pH value, the initial concentration of oxalate and orange I. The optimal C_{ox}^0 for γ-FeOOH, IO-250, IO-320, IO-420 and IO-520 were 1.8, 1.6, 3.5, 3.0 and 0.8 mM, respectively. The photodegradation of orange I in the presence of optimal C_{ox}^0 was ranked as the order of γ-FeOOH > IO-250 > IO-320 > IO-420 > IO-520. The optimal range of initial pH value in the iron oxide–oxalate system was at about 3–4. The variation of pH value, the concentration of Fe^{3+} and Fe^{2+} during the photoreaction were also strongly dependent on the C_{ox}^0 and iron oxides.

Acknowledgments

The work was financially supported by the National Natural Science Foundation of PR China (No. 20377011) and the Natural Science Foundation Key Project of Guangdong province (No. 036533).

References

[1] E.J. Weber, R.L. Adams, Chemical- and sediment-mediated reduction of the azo dye disperse blue 79, Environ. Sci. Technol. 29 (1995) 1163–1170.
[2] H. Zollinger, Color Chemistry: Syntheses, Properties and Applications of Organic and Pigments, VCH, New York, 1987.
[3] I. Arslan, I.A. Balcioglu, D.W. Bahnemann, Advanced chemical oxidation of reactive dyes in simulated dyehouse effluents by ferrioxalate-Fenton/UVA and TiO_2/UVA processes, Dyes Pigm. 47 (2000) 207–218.
[4] K. Tanaka, K. Padermpole, T. Hisanaga, Photocatalytic degradation of commercial azo dyes, Water Res. 34 (2000) 327–333.
[5] C. Walling, Fenton's reagent revisited, Acc. Chem. Res. 8 (1975) 125–131.

[6] D.L. Sedlak, A.W. Andren, Aqueous-phase oxidation of polychlorinated biphenyls by hydroxyl radicals, Environ. Sci. Technol. 25 (1991) 1419–1427.
[7] E. Kusvuran, S. Irmak, H.I. Yavuz, A. Samil, O. Erbatur, Comparison of the treatment methods efficiency for decolorization and mineralization of Reactive Black 5 azo dye, J. Hazard. Mater. 119 (2005) 109–116.
[8] R.G. Zepp, J. Hoigne, H. Bader, Nitrate-induced photooxidation of trace organic chemicals in water, Environ. Sci. Technol. 21 (1987) 443–450.
[9] G.V. Buxton, C.L. Greenstock, W.P. Helman, A.B. Ross, Critical review of rate constants for reactions of hydrated electrons, hydrogen atoms and hydroxyl radicals ($^{\bullet}OH/^{\bullet}O^{-}$) in aqueous solution, J. Phys. Chem. Ref. Data 17 (1988) 513–886.
[10] W.R. Haag, C.C.D. Yao, Rate constants for reaction of hydroxyl radicals with several drinking water contaminants, Environ. Sci. Technol. 26 (1992) 1005–1013.
[11] A. Safarzadeh-Amiri, J.R. Bolton, S.R. Cater, The use of iron in advanced oxidation processes, J. Adv. Oxid. Technol. 1 (1996) 18–26.
[12] W.Z. Tang, R.Z. Chen, Decolorization kinetics and mechanisms of commercial dyes by H_2O_2/iron powder system, Chemosphere 32 (1996) 947–958.
[13] J. Bandara, J. Kiwi, Fast kinetic spectroscopy, decoloration and production of H_2O_2 induced by visible light in oxygenated solutions of the azo dye Orange II, New J. Chem. 23 (1999) 717–724.
[14] J. Kiwi, N. Denisov, Y. Gak, N. Ovanesyan, P.A. Buffat, E. Suvorova, F. Gostev, A. Titov, O. Sarkisov, P. Albers, V. Nadtochenko, Catalytic Fe^{3+} clusters and complexes in nafion active in Photo-Fenton processes. High-resolution electron microscopy and femtosecond studies, Langmuir 18 (2002) 9054–9066.
[15] X. Tao, J. Su, J. Chen, J. Zhao, A novel route for waste water treatment: photo-assisted Fenton degradation of dye pollutants accumulated in natural polyelectrolyte microshells, Chem. Commun. 36 (2005) 4607–4609.
[16] M. Pera-Titus, V. Garcia-Molina, M.A. Baños, J. Giménez, S. Esplugas, Degradation of chlorophenols by means of advanced oxidation processes: a general review, Appl. Catal. B 47 (2004) 219–256.
[17] M.L. Kremer, Mechanism of the Fenton reaction. Evidence for a new intermediate, Phys. Chem. Chem. Phys. 1 (1999) 3595–3605.
[18] M.A.A. Schoonen, Y. Xu, D.R. Strongin, An introduction to geocatalysis, J. Geochem. Explor. 62 (1998) 201–215.
[19] C. Swearingen, S. Macha, A. Fitch, Leashed ferrocenes at clay surfaces: potential applications for environmental catalysis, J. Mol. Catal. A 199 (2003) 149–160.
[20] F.E. Rhoton, J.M. Bigham, D.L. Lindbo, Properties of iron oxides in streams draining the Loess Uplands of Mississippi, Appl. Geochem. 17 (2002) 409–419.
[21] U. Schwertmann, R.M. Cornell, Iron oxides in the laboratory: preparation and characterization, second ed., Wiley–VCH, Weinheim, 2000, pp 14–18.
[22] J.K. Leland, A.J. Bard, Photochemistry of colloidal semiconducting iron oxide polymorphs, J. Phys. Chem. 91 (1987) 5076–5083.
[23] C. Siffert, B. Sulzberger, Light-induced dissolution of hematite in the presence of oxalate. A case study, Langmuir 7 (1991) 1627–1634.
[24] B.C. Faust, R.G. Zepp, Photochemistry of aqueous iron(III)-polycarboxylate complexes: roles in the chemistry of atmospheric and surface waters, Environ. Sci. Technol. 27 (1993) 2517–2522.
[25] J.F. Ma, S.J. Zheng, H. Matsumoto, S. Hiradate, Detoxifying aluminum with buckwheat, Nature 390 (1997) 569–570.
[26] D. Duprez, F. Delanoë, J. Barbier Jr., P. Isnard, G. Blanchard, Catalytic oxidation of organic compounds in aqueous media, Catal. Today 29 (1996) 317–322.
[27] Y.G. Zuo, J. Holgné, Formation of hydrogen peroxide and depletion of oxalic acid in atmospheric water by photolysis of iron(III)-oxalato complexes, Environ. Sci. Technol. 26 (1992) 1014–1022.
[28] M.E. Balmer, B. Sulzberger, Atrazine degradation in irradiated iron/oxalate systems: effects of pH and oxalate, Environ. Sci. Technol. 33 (1999) 2418–2424.
[29] P. Mazellier, B. Sulzberger, Diuron degradation in irradiated, heterogeneous iron/oxalate systems: the rate-determining step, Environ. Sci. Technol. 35 (2001) 3314–3320.
[30] A. Bozzi, T. Yuranova, J. Mielczarski, A. Lopez, J. Kiwi, Abatement of oxalates catalyzed by Fe-silica structured surfaces via cyclic carboxylate intermediates in photo-Fenton reactions, Chem. Commun. 8 (2002) 2202–2203.
[31] C. Liu, Y. Gao, F. Li, J. Lei, G. Zhang, Y. Kuang, Photodegradation of 2-mercaptobenzothiazole in the iron oxides-oxalate system under UVA irradiation, Chin. J. Catal. 27 (2006) 139–145.
[32] C. Paipa, M. Mateo, I. Godoy, E. Poblete, M.I. Toral, T. Vargas, Comparative study of alternative methods for the simultaneous determination of Fe^{3+} and Fe^{2+} in leaching solutions and in acid mine drainages, Mineral Eng. 18 (2005) 1116–1119.
[33] F.B. Li, X.Z. Li, M.F. Hou, K.W. Cheah, W.C.H. Choy, Enhanced photocatalytic activity of Ce^{3+}-TiO_2 for 2-mercaptobenzothiazole degradation in aqueous suspension for odour control, Appl. Catal. A 285 (2005) 181–189.
[34] N. Nadtochenko, J. Kiwi, Photoinduced adduct formation between Orange II and $[Fe^{3+}(aq)]$ or $Fe(ox)_3{}^{3-}$–H_2O_2 photocatalytic degradation and laser spectroscopy, J. Chem. Soc., Faraday Trans. 93 (1997) 2373–2378.
[35] J.K. Leland, A.J. Bard, Photochemistry of colloidal semiconducting iron oxide polymorphs, J. Phys. Chem. 91 (1987) 5076–5083.
[36] B. Sulzberger, H. Laubscher, Reactivity of various types of iron(III) (hydr)oxides towards light-induced dissolution, Mar. Chem. 50 (1995) 103–115.